NONLOCAL RANDOM MOTIONS AND THE TRAPPING PROBLEM

Piotr Garbaczewski, Mariusz Żaba

Institute of Physics, University of Opole
Oleska 48, 45-052 Opole, Poland

(Received December 23, 2014; revised version received January 21, 2015)

Lévy stable (jump-type) processes are examples of intrinsically nonlocal random motions. This property becomes a serious obstacle if one attempts to model conditions under which a particular Lévy process may be subject to physically implementable manipulations, whose ultimate goal is to confine the random motion in a spatially finite, possibly mesoscopic trap. We analyze this issue for an exemplary case of the Cauchy process in a finite interval. Qualitatively, our observations extend to general jump-type processes that are driven by non-Gaussian noises, classified by the integral part of the Lévy–Khintchine formula. For clarity of arguments, we discuss, as a reference model, the classic case of the Brownian motion in the interval.

DOI:10.5506/APhysPolB.46.231
PACS numbers: 05.40.–a, 05.40.Fb, 03.65.Db, 02.50.Ey

1. Motivation

In contrast to the locally defined generator $\Delta = \partial^2/\partial x^2$ of the standard Brownian motion in R, generators of Lévy stable processes are spatially nonlocal. In fact, in the symbolic notation (a fractional power $(-\Delta)^{\mu/2}$ is here replaced by $|\Delta|^{\mu/2}$), we have the $\mu \in (0,2)$-stable generator defined as follows

$$\begin{aligned} -|\Delta|^{\mu/2} f(x) &= \int [f(x+y) - f(x)]\, \nu_\mu(dy) \\ &= \frac{2^\mu\, \Gamma\left(\frac{\mu+1}{2}\right)}{\pi^{n/2} \left|\Gamma\left(-\frac{\mu}{2}\right)\right|} \int \frac{f(y) - f(x)}{|x-y|^{\mu+n}}\, dy\,, \end{aligned} \tag{1}$$

where $x \in R^n$ and $\nu_\mu(dy)$ stands for a (self-defining) Lévy measure $\sim 1/|y|^{\mu+1}$. All above integrations are understood in the sense of the Cauchy principal value and $f(x)$ stands for a function in the domain of that (unbounded) operator.

To set the framework for further discussion, let us mention another (popular, folk) form of the stable generator in the dimensionless notation

$$-|\Delta|^{\mu/2} \equiv \frac{\partial^\mu}{\partial |x|^\mu}\,, \tag{2}$$

and turn over to the tightly constrained (to remain in a spatial trap) Lévy-stable process, whose transport equation is typically [1–4] written in a form mimicking the free motion (quite alike the Brownian case)

$$\partial_t f(x,t) = \frac{\partial^\mu}{\partial |x|^\mu} f(x,t) \tag{3}$$

even though the exterior Dirichlet (absorbing/killing) boundary data are imposed: $f(x,t) = 0$ for $x \leq a$ and $x \geq b$, where $a, b \in R$, $t \geq 0$. We have intentionally replaced the free motion probability density function (pdf) $\rho(x,t)$ by more appropriate (spatially not normalized in $L(R)$) function $f(x,t)$, encoding the killing property. We point out that random processes with absorption/killing induce their own inventory of computable quantities, such as *e.g.* first exit time, killing time, mean transit time *etc.* [1–9].

For the standard (killed) Brownian motion in the interval $D = (a,b) \subset R$, the meaning of the locally defined Laplacian in $\partial_t \rho(x,t) = \Delta \rho(x,t)$, while subject to the very same exterior Dirichlet boundary condition $\rho(x,t) = 0$ on $R \setminus D$, $t \geq 0$ is unaffected by the boundary data. We can evaluate all derivatives of the pdf $\rho(x,t)$ point-wise in D.

To the contrary, the fractional operator $\partial^\mu / \partial |x|^\mu$ cannot be defined locally. A formal definition (1), if restricted to $f(x,t) \neq 0$ for $x \in (a,b)$ only, is inconsistent. The appropriate functional form of the constrained nonlocal operator $|\Delta|^{\mu/2} \to |\Delta|_D^{\mu/2}$, $D = (a,b) \in R$ is definitely lacking in the physics-oriented literature. For a mathematical viewpoint on this issue, see *e.g.* [10, 11].

Somewhat disregarded point is that the constrained motion generators determine a corresponding semigroup dynamics through a semigroup kernel given in the familiar Feynman–Kac form. We shall explore this property in below to pass to nonlocally defined random motions which *do* preserve a pdf ρ normalization, while inheriting the constraints (*e.g.* being trapped in D), by following the line of research developed in Refs. [12–16].

2. What is meant by the Brownian motion in the interval?

2.1. Schrödinger semigroup transcript of the Fokker–Plack dynamics

Before embarking on the problem of jump-type processes in a spatially finite trap, let us invoke a a classic exercise ([17], Section 5.5.3, page 110) illustrating a method of solution of the Fokker–Planck equation in one variable, by means of so-called eigenfunction expansions. The major step there is a transformation of the Fokker–Planck operator into a Hermitian operator (which, subsequently, needs to be elevated to the self-adjoint or essentially self-adjoint operator status [18]). Told otherwise, the Fokker–Planck equation is solved by passing to an associated Schrödinger-type equation. No imaginary unit appears here and thence, we deal not with a unitary evolution, but with the semigroup dynamics.

The essence of the method (we consider the 1D case, in a dimensionless notation) lies in passing from the Fokker–Planck equation

$$\partial_t \rho = \Delta \rho - \nabla \left(b\, \rho \right), \tag{4}$$

for the probability density function $\rho(x,t)$, with the initial condition $\rho_0(x) = \rho(x,0)$ and suitable boundary data, where the existence of the stationary (equilibrium) pdf $\rho(x,t) \to \rho_*(x)$ is presumed to be granted in the large time asymptotic, to the Schrödinger-type equation *i.e.* the semigroup $\exp(-Ht)$

$$\partial_t \Psi = -H\Psi = \Delta\Psi - \mathcal{V}\Psi\,, \tag{5}$$

for a real-valued function $\Psi(x,t)$. We tacitly presume the potential to be confining so that the positive definite ground state $\psi(x) \doteq \rho_*^{1/2}(x)$ exists and corresponds to the 0 eigenvalue of H. This can be always achieved by subtracting the lowest non-zero eigenvalue of H, if actually in existence, from the potential.

The auxiliary potential $\mathcal{V}$, up to an additive constant, takes the form (actually obeys the compatibility condition, given $\rho_*(x)$)

$$\mathcal{V}(x) = \rho_*^{-1/2} \Delta \rho_*^{1/2}\,. \tag{6}$$

The transformation between (4) and (5) is executed by means of a substitution (remember that $\rho(x,t)$, as a probability density function, integrates to 1)

$$\rho(x,t) = \Psi(x,t)\rho_*^{1/2}(x)\,. \tag{7}$$

Another expression for the Schrödinger potential reads $\mathcal{V} = b^2/2 + \nabla b$, where $b = \nabla \ln \rho_*$, thus completing the mapping.

Solving (5), with the ground state of H in hands, we readily get a solution $\rho(x,t)$ of the Fokker–Planck equation which equilibrates to $\rho_*(x)$. The technical advantage of the transformation (7) is that we, in fact, can recover a complete spectral solution for H, which determines an associated semigroup (Feynman–Kac) kernel. The latter, after accounting for the ground state $\rho_*^{1/2}$ and the so-called Doob's transformation, determines, in turn, the transition probability density of the diffusion process in question (*i.e.* that underlying (4)), see *e.g.* Refs. [5, 6, 13, 17]. Another technical advantage is that even quite complicated Fokker–Planck dynamics, specifically with no available analytic solution, can be addressed by means of powerful and fairly accurate numerical algorithms, invented for the Schrödinger-type (Euclidean, *i.e.* semigroup) evolution problems [19, 20].

2.2. Risken's infinite well

In conjunction with the Brownian motion in the interval say $D=(-1,1)$, the infinite square well potential, with $V(x)=0$ for $x\in(-1,1)\subset R$, is hereby chosen as a mathematical encoding of the Laplacian with the Dirichlet boundary conditions (so-called zero exterior condition on $R\setminus D$) imposed on $L^2([-1,1])$ functions $\psi(x)$ in its domain: $\psi(x)=0$ for $|x|\geq 1$.

The spectral solution is well known. In particular, we readily have in hands the lowest eigenvalue $\pi^2/4$ and the ground state function $\cos(\pi x/2)$ of the operator $-\Delta$, whose action is restricted to the well interior.

The orthonormal eigenbasis is composed of functions $\psi_n(x)$, $n=1,2,\ldots$ such that $\psi(x)=0$ for $|x|\leq a$, where n labels positive eigenvalues $E_n\sim n^2$. More explicitly: $\psi_n(x)=\cos(n\pi x/2)$ for n even and $\sin(n\pi x/2)$ for n odd, while the eigenvalues read $E_n=(n\pi/2)^2$.

It is clear that any $\psi\in L^2([-1,1])$, in the domain of the infinite well Hamiltonian, may be represented as $\psi(x)=\sum_{n=1}^{\infty}c_n\psi_n(x)$. Its time evolution follows the Schrödinger semigroup pattern $\psi(x)\to\Psi(x,t)=[\exp(-Ht)\psi](x)=\sum_{n=1}^{\infty}c_n\exp(-E_nt)\,\psi_n(x)$.

Let us consider $H=-\Delta-E_1$ instead of $H=-\Delta$ proper (the boundary data being implicit). Accordingly, the *a priori* positive-definite ground state $\psi_1(x)\doteq\rho_*^{1/2}(x)$ corresponds to the zero eigenvalue of $H-E_1$. Thence, the "renormalized" semigroup evolution reads $\Psi(x,t)=\exp(+E_1t)\sum_{n=1}^{\infty}c_n\exp(-E_nt)\,\psi_n(x)\to\psi_1(x)=\rho_*^{1/2}(x)$. Here, in a self-explanatory notation, we have defined the probability density function (pdf) $|\psi_1(x)|^2=\rho_*(x)$ which is an equilibrium solution of the associated Fokker–Planck equation.

The semigroup kernel $\exp(-tH)(x,y)$, associated with such H whose lowest eigenvalue is 0, defines a time homogeneous random process in the interval. Its standard spectral representation is (the renormalization by $-E_1$ produces here an exponential factor), see also [9]

$$
\begin{aligned}
k(t,x,y) &= \exp(-Ht)(x,y) \\
&= \exp\left(+\pi^2 t/4\right) \sum_{n=1}^{\infty} \exp\left[-(n\pi/2)^2\, t\right]\ \psi_n(x)\, \psi_n(y) \\
&= \sum_{n=1}^{\infty} \exp\left[\left(1-n^2\right) \pi^2\, t/4\right] \sin[n\pi(x+1)/2]\, \sin[n\pi(y+1)/2]\,. \qquad (8)
\end{aligned}
$$

Here, $\Psi(x,t) = \int k(t,x,y)\Psi_0(y)\, dy$. In probabilistic terms, the kernel allows to define a conditional probability $P_x(X_t) = k(t,x,y)dy$ that a process started at x will reach a vicinity dy of y in time t.

In the standard lore of the Brownian motion with killing (sometimes identified with absorption), one adds that t is prior to a killing time τ. An inventory of typical calculable functions/functionals related to the killed Brownian motion (various forms of the transition density k, distribution function and density of first exit time τ, mean first passage/exit time, *etc.*) can be found in [1, 7–9].

2.3. Fokker–Planck dynamics in the interval

Under the very same infinite well conditions, after taking account of (5)–(7), another random process (devoid of any killing notion) is defined by means of the regular transition probability density (here a multiplicative Doob's transformation is involved [13]; x and y belong to an open interval D)

$$
p(t,x,y) = k(t,x,y)\frac{\rho_*^{1/2}(x)}{\rho_*^{1/2}(y)} \qquad (9)
$$

so that a consistent propagation of the Fokker–Planck probability density function is secured: $\rho(x,t) = \int p(t,x,y)\, \rho_0(y)\, dy$ entirely within the interval $D \subset R$. More details on these and related issues can be found in [13, 17], see also [5].

The Fokker–Planck equation (4), with a stationary solution $\rho_*(x)$, can be rewritten in the form of the general transport equation

$$
\partial_t \rho = \left[\rho_*^{1/2} \Delta \left(\rho_*^{-1/2}\, \cdot\right) - \rho_*^{-1/2} \left(\Delta \rho_*^{1/2}\right)\right] \rho \qquad (10)
$$

with the (motion in the interval) boundary data being implicit.

Remark 1: This equation often happens to be explicitly written in terms of $\rho_*(x) = \exp[-\Phi(x)]$, where Φ plays the role of the Boltzmann–Gibbs potential. In Ref. [15], we have introduced a thermal redefinition of the equilibrium pdf (self-explanatory notation): $\rho_*(x) = (1/Z)\exp[-V(x)/k_{\mathrm{B}}T]$, see also [15].

Remark 2: The transport equation (10) is amenable to an immediate generalization to non-Gaussian noises, *c.f.* [14, 15]. Anticipating further discussion, we note that a seemingly "naive" replacement of Δ by a fractional generator $-|\nabla|^\mu$, where $\mu \in (0,2)$ is a stability index, produces the fractional transport equation whose dynamics stems form that for the related fractional semigroup, [14, 15, 21, 22]. A particular choice of $\mu = 1$ refers to the Cauchy case. In contrast to the Brownian motion, the emergent non-Gaussian (here fractional) transport equation cannot be reduced to any known Fokker–Planck form, see *e.g.* [14, 15, 23] and compare with [12, 24]. A proper handling of constraints in the nonlocal random dynamis (*e.g.* motion in the interval) is a subject of our subsequent analysis.

2.4. Relaxing the boundary data: Brownian motion in (and in the vicinity of) a finite well

Following the previous Risken's recipe, let us consider the Brownian motion in and around the finite well. We shall be interested in a sequence of deepening finite wells and the validity of an infinite well approximation for wells that are sufficiently deep. By passing to the finite well, we relax the "rigid" Dirichlet boundary data, since now the pdf tails always persist even far beyond the well boundaries.

Let us consider $T = -\Delta$ and $\mathcal{V}$ such that $\mathcal{V}(x) = 0$ for $|x| < 1$, while $\mathcal{V}(x) = V_0 > 0$ for $|x| \geqslant 1$. The spectral solution for $H = T + \mathcal{V}$ is a classic exercise again. In 1D, there exists at least one bound (ground) state and a substantial part of the energy spectrum is continuous.

The eigenvalue problem $H\psi(x) = E\psi(x)$ allows to identify at least one (ground state) eigenvalue and the ground state itself. Namely, the ground state comes from

$$\psi_0(x) = \begin{cases} A\cos(\kappa)e^{k(x+1)}\,, & x < -1 \\ A\cos(\kappa x)\,, & -1 \leqslant x \leqslant 1 \\ A\cos(\kappa)e^{k(1-x)}\,, & x > 1 \end{cases}\,, \tag{11}$$

where

$$\kappa = \sqrt{E}\,, \qquad k = \sqrt{V_0 - E}\,, \qquad A = \sqrt{\frac{k}{k+1}} \tag{12}$$

and E must be the least real number obeying

$$\begin{cases} k = \kappa\tan(\kappa) \\ \kappa^2 + k^2 = V_0 \end{cases}\,. \tag{13}$$

The ground state eigenvalues $E = E_1$ for various well depths have been

obtained numerically and we reproduce them up to four decimal digits

$$\begin{array}{ll} V_0 = 5\,, & E_1 = 1.1475\,, \\ V_0 = 20\,, & E_1 = 1.6395\,, \\ V_0 = 500\,, & E_1 = 2.2605\,, \\ V_0 = 1000\,, & E_1 = 2.3184\,, \\ V_0 = 5000\,, & E_1 = 2.3989\,, \\ V_0 = 50000\,, & E_1 = 2.4296\,, \\ V_0 \sim \infty\,, & E_1 = \pi^2/4 \sim 2.4674\,. \end{array} \tag{14}$$

We note that $H - E_1$ has 0 as the lowest eigenvalue, the ground state being identified by setting $E = E_1$ in Eq. (9).

To avoid the risk of confusion, we point out that subsequently the notation H is employed for the "renormalized" Hamiltonian $H - E_1$. We denote $\rho_*^{1/2} = \psi_0$, where $H\rho_*^{1/2} = 0$ and, in accordance with [14, 21], define the time evolution generator in $\partial_t \rho = L\rho$ as $L = -\rho_*^{1/2} H \rho_*^{-1/2}$. This implies the validity of the transport equation (10) which, in turn, stands for both *(i)* the rewriting of the Fokker–Planck equation and *(ii)* the direct consequence of the semigroup evolution (5), see *e.g.* also [15].

Functional shapes of finite well ground states have been obtained numerically (details of the algorithm, inferred from [19, 20], are available upon request) and results are depicted in Fig. 1. The displayed finite well ground states show up a conspicuous (here graphical/visual) convergence trend towards the infinite well ground state $\cos(\pi x/2)$. The ground state tails appear to be relevant for shallow wells.

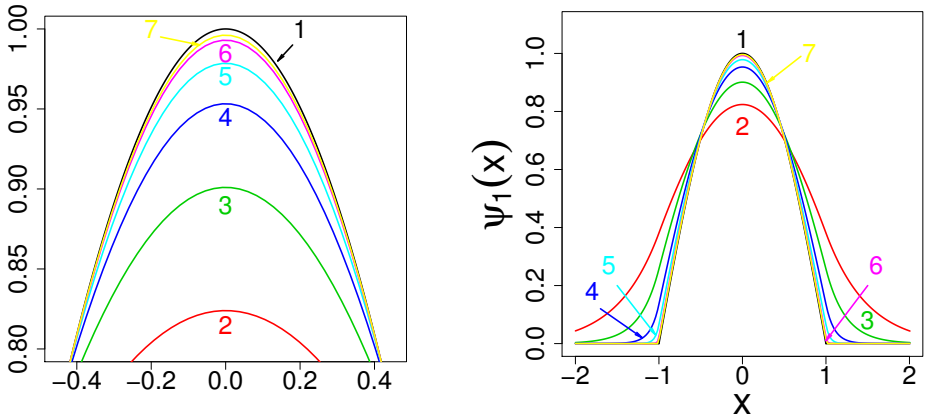

Fig. 1. Ground states $\rho_*^{1/2}$ for a sequence of deepening finite wells. Numbers refer to: 1 — $\cos(\pi x/2)$, while $2, 3, 4, 5, 6, 7$ enumerate well depths $V_0 = 5$, 20, 100, 500, 5000, 50000, respectively. Left panel shows an enlargement of the vicinity of maxima.

Let us recall that, in accordance with (1)–(4), given the ground state of (2) and the semigroup-driven evolution of $\Psi(x,t)$, we have readily defined the pdf of the Brownian motion without killing, albeit asymptotically (almost) trapped in the finite well. Indeed, we have $\rho(x,t) = \Psi(x,t)\rho_*^{1/2}(x)$ and the time evolution of $\rho(x,t)$ is fully compatible with the Fokker–Planck equation (1). To visualize the finite well dynamics in its Fokker–Planck transcript, let us consider the standard Gaussian as an initial pdf: $\rho_0(x) = \frac{1}{\sigma\sqrt{2\pi}}\exp(-(x-\mu)^2/2\sigma^2)$, where we set $\mu = 0$, $\sigma = 2$. See, *e.g.* Fig. 2.

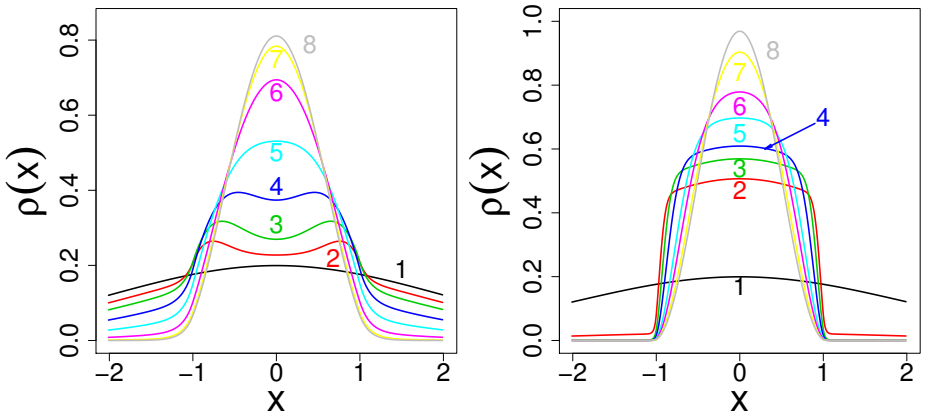

Fig. 2. Fokker–Planck dynamics of $\rho(x,t)$ in a finite well environment. It is started from the Gaussian with cutoffs mentioned in the text. Numbers refer to: 1 — the Gaussian (initial data), $2, 3, 4, 5, 6, 7$, depict the $\rho(x,t)$ evolution at selected respective time instants (number of algorithm iteration steps). Left panel: for $V_0 = 20$, we have depicted time instants $4000, 8000, 15000, 25000, 40000, 60000$, and the vicinity of an asymptotic (8) for 120000. Right panel: for $V_0 = 1000$, the evolution proceeds somewhat faster and we have, respectively, $300, 600, 1200, 3000, 5000, 10000$, while 8 refers to 100000. The time increment equals $\Delta t = 10^{-5}$.

Remark 3: The transport equations (4) and (10) can be rewritten as $\partial_t \rho = L\rho$ where the operator L reads: $L = -\rho_*^{1/2} H \rho_*^{-1/2}$. The dynamics of $\rho(z,t)$ can be simulated by employing the standard finite difference scheme. Namely, for a sufficiently small time increment Δt, we can set $\rho(x, t+\Delta t) \approx \rho(x,t) + \Delta t\,(L\rho)(x,t)$. In the Brownian case, $\Delta t = 10^{-5}$ is a reliable choice. After each simulation step, the outcome needs to be normalized to yield a consistent approximation $\rho(x, k\Delta t)$, $k = 0, 1, 2, \ldots$ of the probability density function at the time instant $k\Delta t$.

Remark 4: To facilitate numerical computations (optimize the time necessary to get close to the equilibrium pdf), in the case of wells with $V_0 = 500$ and $V_0 = 1000$, the support of the Gaussian is restricted to $[-10, 10]$ which is followed by the $L^2(R)$ normalization of the outcome. In the case of shallow wells, $[-a, a]$ with $a = 50$ has been employed for $V_0 = 20$, while $a = 150$ for $V_0 = 5$. Clearly, time (in terms of the computer algorithm, it is the number of steps) necessary to reach the vicinity of an equilibrium is considerably longer for shallow wells.

3. Cauchy process in (and in the vicinity of) the finite well

3.1. Finite Cauchy wells

Our major point of interest is an exemplary nonlocal Cauchy jump-type process, that is constrained to "live" exclusively within the interval $(-1, 1) \subset R$, due to killing (absorption) at the boundaries, according to the traditional probabilistic lore, [11–22]. In the mathematical literature, the process is considered in the finite interval, as a problem for itself. We wish to maintain at least a residual link with physical intuitions about trapping mechanism. In particular, it may be illuminating to have in hands a model which shows how long jumps can be tamed, with an ultimate reduction of their impact once we approach the motion restricted to the interval only.

To this end, let us introduce somewhat milder boundary conditions (permitting arbitrarily long jumps to occur; note that in numerical procedures their length needs to be bounded by a certain $a > 0$), by referring to a sequence of deepening but finite Cauchy wells. Spectral solutions for sufficiently deep wells may be satisfactorily approximated by that for the infinite one, see *e.g.* [11] and Fig. 3. For finite wells, there are no *a priori* limitations upon the size of jumps in the pertinent jump-type process and the R-nonlocality of the problem persists, while for the infinite well its impact is limited to the interior of $D \subset R$.

We have in hands [22] numerical tools allowing to deduce the corresponding ground states (actually approximants of the "true" ones) and the semigroup dynamics of $\Psi(x, t)$ in the finite well regime. A family of related pdfs $\rho(x, t)$; $t \geq 0$ readily follows by employing the transformation (7). The inferred probability density functions (pdfs) are driven towards equilibrium by a suitable master equation. We point out that, in contrast to the Brownian motion of Section 2, this equation cannot be reduced to any known Langevin-based form of the fractional Fokker–Planck equation [14, 15, 23, 24].

In the finite well (semigroup) regime, a family of jump-type processes running in sufficiently deep wells, admits only the residual tails of the equilibrium pdf to persist beyond the trap (*e.g.* $D = (-1, 1)$) interior. A degree of an approximation accuracy, with which the infinite well data are repro-

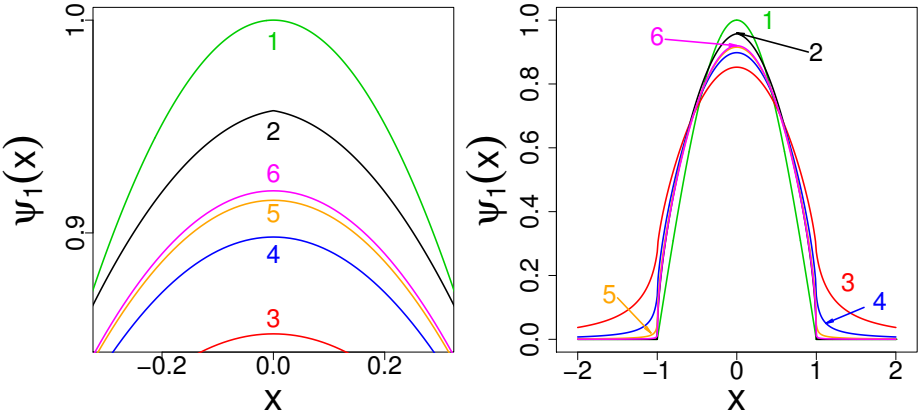

Fig. 3. Ground state solution of the finite Cauchy well. Numbers refer to: 1 — $\cos(\pi x/2)$, 2 — an approximate solution, Eq. (13) in [11], $3, 4, 5, 6$ refer to the well depths, respectively $5, 20, 100, 500$. Convergence symptoms (towards an infinite well solution) are visually identifiable. Left panel reproduces an enlarged resolution around the maximum of the ground state.

duced, is quantified in terms of deviations of each equilibrium pdf from that emerging in the reference $(-1, 1) \subset R$ trapping model. This model we have investigated before, [22], see also [11]. It is the complete "blockade" of long jumps, that ultimately calls for giving a meaning to the Dirichlet-constrained nonlocal generator $|\nabla|_D$, where $D = (-1, 1)$.

We consider the Cauchy–Schrödinger semigroup dynamics $\exp(-Ht)$, where $H = T + V - E_1$ and $-T$ stands for the Cauchy generator, *e.g.* $T = |\nabla| = (-\Delta)^{1/2}$, while V denotes the finite well potential defined in Section 2.4 and E_1 is the bottom (ground state) eigenvalue of H. Here

$$T\,\psi(x) = (-\Delta)^{1/2}\,\psi(x) = \frac{1}{\pi}\int \frac{\psi(x) - \psi(x+z)}{z^2} dz\,, \tag{15}$$

and the integral is interpreted in terms of the Cauchy principal value.

The semigroup evolution gives rise to the transport equation for $\rho(x,t) = \Psi(x,t)\rho_*^{1/2}(x)$, which is a straightforward generalization of Eq. (10) mentioned in Remark 2, see for more details [12, 15, 21]

$$\partial_t \rho = -\left[\rho_*^{1/2} T\,\left(\rho_*^{-1/2}\cdot\right) - \rho_*^{-1/2}\left(T\rho_*^{1/2}\right)\right]\rho\,, \tag{16}$$

where $\rho_*^{1/2}$ is the $L^2(R)$ normalized ground state of $H = T + V - E_1$, associated with the eigenvalue 0.

Remark 5: Our work mostly concentrates on mathematical aspects of the trapping problem. It is useful to turn the reader's attention to other, than trapping proper, physical features of the involved formalism. The Lévy flight model as described by the Lévy–Schrödinger semigroup may be essentially identified with the topologically-induced Lévy flight of Ref. [14]. That model is relevant for describing diffusion of polymers in the limit of fast conformational changes. Another point worth stressing is the fact that the equilibrium pdf of particle positions is connected with the Lévy–Schrödinger operator ground state wave function (we take it always to be nonnegative and thence use the notation $\rho_*^{1/2}$). The ground state existence is always granted, if the semigroup operator (and its generator) has at least one isolated lowest eigenvalue, or has a discrete component in its spectrum. One more useful observation is that the pertinent ground state (after squaring) gives rise to the Boltzmann equilibrium pdf ρ_* for the corresponding effective potential, *c.f.* Remark 1 and [14].

We have numerically recovered the finite Cauchy well ground (and higher energy) states for various wells depths in Ref. [22]. A suitable algorithm (based on the Strang splitting method) has been implemented there for the semigroup evolution of $\Psi(x,t)$, including an issue of its large time asymptotic $\rho_*^{1/2}$. As a consequence, we can readily deduce the evolution of the inferred pdf $\rho(x,t) = \Psi(x,t)\rho_*^{1/2}(x)$ whose asymptotic $\rho_*(x)$ actually is.

We recall [14–16] that the transport equation (16) cannot be reduced to any traditional form of the Langevin-based fractional Fokker–Planck equation, like those discussed in Refs. [23, 24].

Analytic outcomes are generically beyond the reach and the computer assistance is unavoidable in the present context. Various technical details of developed numerical routines are skipped in the present paper, see *e.g.* [22]. It is useful to mention that integrations involved in the definition of the Cauchy generator need to be chosen finite, to optimize computations. In view of the preselected trap size $D = (-1,1)$, a reliable cutoff for the integration domain is $x \in [-a,a]$, with $a = 50$. We have analyzed before [22] a sensitivity of computed eigenvalues (high) and eigenfunction shapes (low) on the cutoff parameter a.

In the Cauchy case, we set a time increment $\Delta t = 10^{-3}$, which is 100 times longer than that adopted for the Brownian case. While attempting any comparison of Brownian and Cauchy outcomes, one needs to remember that *e.g.* 100 Cauchy algorithmic steps correspond to time 10^{-1} and this time instant, in turn, does correspond to 10000 algorithmic steps in the Brownian case.

Figures (4) and (5) provide a visualization, in terms of $\rho(x,t)$ that has been started from a Gaussian, of how the entrapping of the Cauchy process takes place in the $(-1,1)$ finite well environment. We have depicted both

shallow ($V_0 = 5, 20$) and deep ($V_0 = 500$) wells. The term "asymptotic" refers to time regimes such that the resultant "asymptotic curve" cannot be distinguished from an independently obtained stationary $\rho_*(x)$. At least within the adopted graphical resolution.

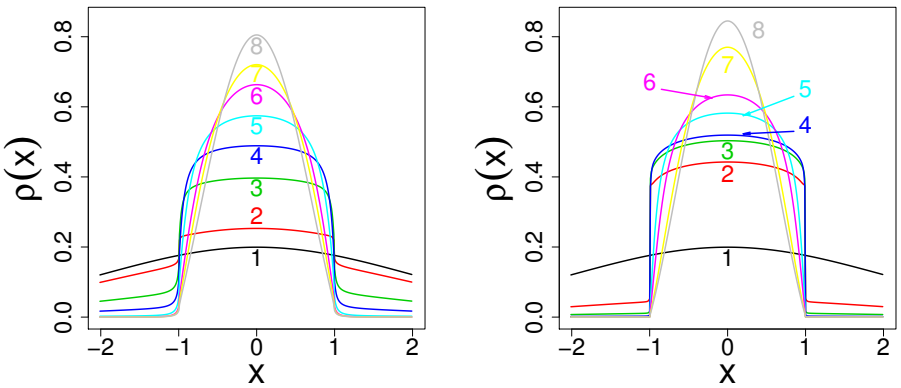

Fig. 4. Cauchy evolution of $\rho(x,t)$ in the finite well environment. Left panel $V_0 = 20$: numbers refer to: 1 — initial Gaussian pdf, $2, 3, 4, 5, 6, 7$, algorithmic time instants after $10, 50, 100, 200, 400, 600$ steps, 8 — a close vicinity of an asymptotic pdf is approached after 2500 steps. Right panel $V_0 = 500$: 1 — initial Gaussian pdf, $2, 3, 4, 5, 6, 7$, refer to $2, 4, 6, 100, 200, 600$ algorithm steps respectively, 8 — a vicinity of an asymptotic pdf after 2000 steps. Time increment $\Delta t = 10^{-3}$ is 100 times larger than that adopted for Brownian simulations.

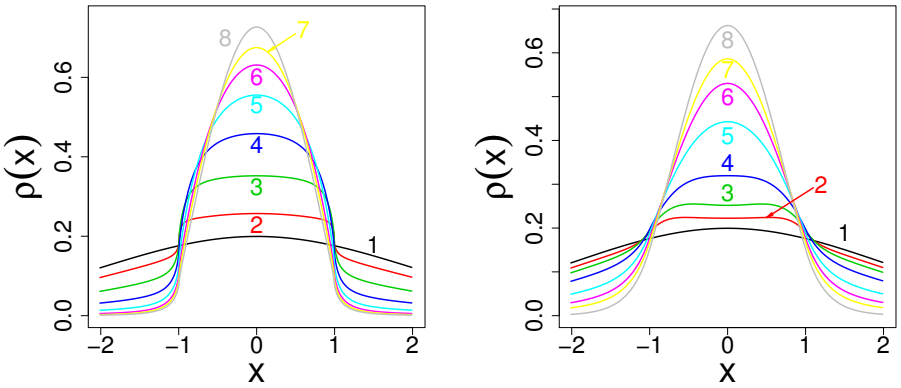

Fig. 5. Cauchy evolution *versus* Brownian evolution of $\rho(x,t)$ in the finite well environment, $V_0 = 5$. Left panel: Cauchy driver, 1 — initial Gaussian pdf, $2, 3, 4, 5, 6, 7$, refer to algorithmic time instants set by $50, 150, 300, 500, 750, 1000$ steps, while 8 to an asymptotic retrieved after 3000 steps. Here $\Delta t = 10^{-3}$. Right panel: Brownian driver, 1 — initial Gaussian pdf, $2, 3, 4, 5, 6, 7$ refer to algorithmic time instants set by $5000, 10000, 20000, 40000, 60000$ steps, with an asymptotic 8 approached after 150000 steps. Here $\Delta t = 10^{-5}$.

In Fig. (6) we compare Cauchy and Brownian trapping scenarios in a shallow well $V_0 = 5$ environment.

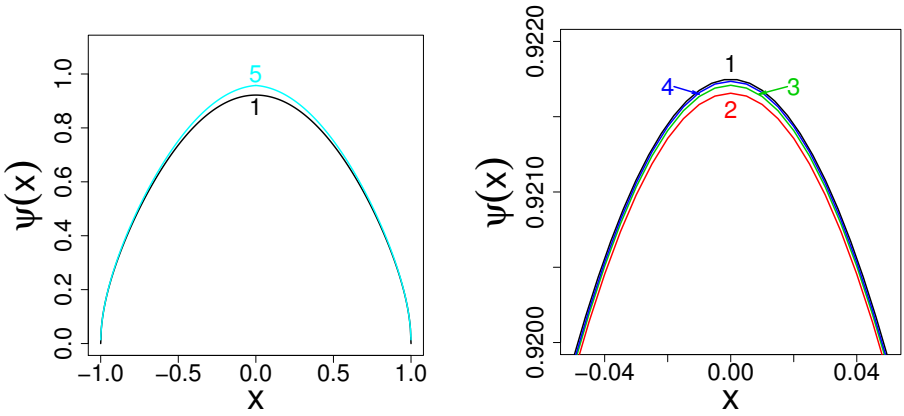

Fig. 6. Ground states for deep Cauchy wells. Numbers denote: 1 — our analytic proposal $\psi(x)$ for the infinite well, 2,3,4 — well depths $V_0 = 5000, 10000, 20000$ respectively, 5 — an approximation of the infinite well ground state proposed in Ref. [11]. Notice that in the right panel, where an enlargement around the maxima is depicted, the approximating curve 5 could not be fit to the current panel area, in view of adopted fine resolution scales.

3.2. Infinite Cauchy well: ground state function problem

In the case of the Cauchy well, our numerical algorithm allows to deduce approximate eigenvalues and eigenfunctions of the pertinent spectral problem. Since an infinite well limit, to which we continually refer, can be formulated *solely* in terms of $L^2([-a,a])$ (see however [18] for another viewpoint in the local context), we may quite intentionally consider an orthonormal basis in $L^2[-1,1]$, subject to a trivial extension to $L^2(R)$

$$\Phi^{(0)}_{n=2m+1}(x) = \begin{cases} A\cos\left(\frac{n\pi x}{2}\right), & |x|<1, \\ 0, & |x|\geqslant 1, \end{cases}$$

$$\Phi^{(0)}_{n=2m}(x) = \begin{cases} A\sin\left(\frac{n\pi x}{2}\right), & |x|<1, \\ 0, & |x|\geqslant 1, \end{cases} \qquad m=0,1,\ldots \tag{17}$$

The normalization constant A equals ± 1. Generically, a particular sign choice seems to have no physical meaning. However, in view of our semigroup discussion, we adopt $A = 1$ which secures that an asymptotic $\Psi(x,t) \to \rho_*(x)$ has an unambiguous meaning. The above trigonometric functions actually stand for a complete set of eigenfunctions of the Brownian infinite well problem.

In the fractional (like *e.g.* Cauchy) context, many authors have claimed that trigonometric functions should be close to the "true" eigenfunctions of fractional semigroups in the interval. See, *e.g.* [11, 15, 22] for a brief summary of statements and pitfalls related to this issue. One can possibly accept a statement that for sufficiently large n, the eigenvalues are close to $E_n = n\pi/2$ and eigenfunctions are close to the above trigonometric basis system in $L^2([-1,1])$.

As yet no explicit analytic formula for any fractional semigroup ground state in the infinite well is available. Approximate analytic expressions of a relatively good finesse are known. This statement extends to the eigenvalues as well. Coming back to the Cauchy infinite well problem with boundaries at the ends of $[-1,1]$, we note that for low lying eigenvalues, the formula $E_n = n\pi/2$ is plainly wrong. Actually, we have (it is still an analytic approximation, provided n is not too small — in fact $n > 10$ does the job) [11]

$$E_n = \frac{n\pi}{2} - \frac{\pi}{8} + O\left(\frac{1}{n}\right) . \tag{18}$$

In [22], we have deduced numerically the Cauchy infinite well eigenvalues, together with shapes of the corresponding eigenfunctions. The level of accuracy for low lying eigenstates is surprisingly good.

For completeness of arguments, let us give an explicit expression for approximate eigenfuctions associated with the infinite Cauchy well. Namely, we have (with minor adjustments of the original notation of Ref. [11])

$$\psi_n(x) = q(-x)F_n(1+x) - (-1)^n q(x)F_n(1-x)\,, \qquad x \in R\,, \tag{19}$$

where $E_n = \frac{n\pi}{2} - \frac{\pi}{8}$ and $q(x)$ is an auxiliary function

$$q(x) = \begin{cases} 0 & \text{for } x \in \left(-\infty, -\frac{1}{3}\right), \\ \frac{9}{2}\left(x+\frac{1}{3}\right)^2 & \text{for } x \in \left(-\frac{1}{3}, 0\right), \\ 1 - \frac{9}{2}\left(x-\frac{1}{3}\right)^2 & \text{for } x \in \left(0, \frac{1}{3}\right), \\ 1 & \text{for } x \in \left(\frac{1}{3}, \infty\right). \end{cases} \tag{20}$$

The function $F_n(x)$ is defined as follows: $F_n(x) = \sin\left(E_n\, x + \frac{\pi}{8}\right) - G(E_n\, x)$, where $G(x)$ is the Laplace transform $G(x) = \int_0^\infty e^{-xs}\gamma(s)ds$ of a positive definite function $\gamma(s)$

$$\gamma(s) = \frac{1}{\pi\sqrt{2}}\frac{s}{1+s^2}\exp\left(-\frac{1}{\pi}\int_0^\infty \frac{1}{1+r^2}\log(1+rs)dr\right) . \tag{21}$$

Evidently, things are here much more complicated than an oversimplified (deceiving but faulty) guess (16) would suggest.

Since it is the ground state that matters in our discussion of the inferred pdf $\rho(x,t)$ dynamics, let us introduce another analytic approximation of the "true" ground state in the Cauchy case. Namely, while skipping a number of detailed hints that motivate our choice, we propose the following function as the pertinent approximation

$$\psi(x) = C\sqrt{(1-x^2)\cos(\alpha x)}\,, \tag{22}$$

where

$$\alpha = \frac{1443}{4096}\pi = \left(\frac{\pi}{2} - \frac{\pi}{8}\right) - \frac{\pi}{64} - \frac{\pi}{256} - \frac{\pi}{512} - \frac{\pi}{1024} - \frac{\pi}{4096} \tag{23}$$

and $C = 0.921749$ is a normalization constant. We note that the boundary behavior of our ψ conforms with that predicted by means of scaling arguments in [2], *e.g.* drops down to 0 as $(1-|x|)^{1/2}$. Clearly, ψ becomes close to the cosine once away from the boundaries of $[-1,1]$. The function is concave and conforms with earlier mathematical results on the ground state shape for stable generators in the interval [25, 26].

The approximation accuracy with which our $\psi(x)$ mimics the numerically obtained very deep (and ultimately the infinite) Cauchy well ground states seems to be much better than that offered by the analytic proposal of [11], see *e.g.* Figs. (6) and (7).

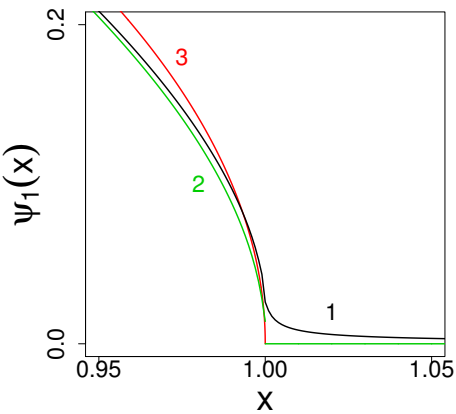

Fig. 7. Finite *versus* infinite Cauchy well ground state in the vicinity of the boundary +1 of $[-1,1]$: 1 (black) — the algorithm outcome for the finite $V_0 = 500$ well, 2 (green) — an approximate infinite well expression from Ref. [11], 3 (red) — an approximate form of $\psi_1(x) \sim (1-|x|)^{1/2}$, in the vicinity of the infinite well barriers, as proposed in Ref. [2].

REFERENCES

[1] B. Dybiec, E. Gudowska-Nowak, P. Hänggi, *Phys. Rev.* **E73**, 046104 (2006).

[2] A. Zoia, A. Rosso, M. Kardar, *Phys. Rev.* **E76**, 021116 (2007).

[3] P.M. Drysdale, P.A. Robinson, *Phys. Rev.* **E58**, 5382 (1996).

[4] S.V. Buldyrev *et al.*, *Physica A* **302**, 148 (2001).

[5] W.G. Faris, *Diffusive Motion and Where It Leads*, in: W.G. Faris (Ed.), *Diffusion, Quantum Theory and Radically Elementary Mathematics*, Princeton University Press, Princeton 2006.

[6] E.B. Davies, *Heat Kernels and Spectral Theory*, Cambridge University Press, Cambridge 1990.

[7] S. Redner, *A Guide to First-passage Processes*, Cambridge University Press, Cambridge 2001.

[8] A.N. Borodin, P. Salminen, *Handbook of Brownian Motion — Facts and Formulae*, Birkhäuser, Basel 2002.

[9] A. Lejay, A library of simulating Brownian motion's exit times and positions from simple domains, Rapport technique No. 7523, INRIA, Nancy 2011.

[10] T. Kulczycki, M. Kwaśnicki, J. Małecki, A. Stós, *Proc. London Math. Soc.* **101**, 589 (2010).

[11] M. Kwaśnicki, *J. Funct. Anal.* **262**, 2379 (2012).

[12] P. Garbaczewski, *Acta Phys. Pol. B* **43**, 977 (2012).

[13] P. Garbaczewski, R. Olkiewicz, *J. Math. Phys.* **37**, 732 (1996).

[14] D. Brockmann, I.M. Sokolov, *Chem. Phys.* **284**, 409 (2002).

[15] P. Garbaczewski, V.A. Stephanovich, *Physica A* **389**, 4419 (2010).

[16] P. Garbaczewski, V.A. Stephanovich, *Phys. Rev.* **E84**, 011142 (2011).

[17] H. Risken, *The Fokker–Planck Equation*, Springer-Verlag, Berlin 1989.

[18] P. Garbaczewski, W. Karwowski, *Am. J. Phys.* **72**, 924 (2004).

[19] P. Bader, S. Blanes, F. Casas, *J. Chem. Phys.* **139**, 124117 (2013).

[20] J. Auer, E. Krotschek, *J. Chem. Phys.* **115**, 6841 (2001).

[21] P. Garbaczewski, V. Stephanovich, *J. Math. Phys.* **54**, 072103 (2013).

[22] M. Żaba, P. Garbaczewski, *J. Math. Phys.* **55**, 092103 (2014).

[23] I. Eliazar, J. Klafter, *J. Stat. Phys.* **111**, 739 (2003).

[24] S. Jespersen, R. Metzler, H.C. Fogedby, *Phys. Rev.* **E59**, 2736 (1999).

[25] R. Bañuelos, T. Kulczycki, *J. Funct. Anal.* **211**, 355 (2004).

[26] R. Bañuelos, T. Kulczycki, P.J. Mendez-Hernandez, *Potential Anal.* **24**, 205 (2006).